AGU100 ADVANCING EARTH AND SPACE SCIENCE

Geophysical Research Letters

RESEARCH LETTER
10.1029/2019GL082743

Low Frequency Radio Pulses Produced by Terrestrial Gamma-Ray Flashes

Yunjiao Pu[1], Steven A. Cummer[1], Fanchao Lyu[1,2], Michael Briggs[3], Bagrat Mailyan[4], Matthew Stanbro[4], and Oliver Roberts[4]

[1]Electrical and Computer Engineering Department, Duke University, Durham, NC, USA, [2]Now at Department of Building Service Engineering, The Hong Kong Polytechnic University, Hung Hom, Hong Kong, [3]Center for Space Plasma and Aeronomic Research, University of Alabama in Huntsville, Huntsville, AL, USA, [4]Universities Space Research Association, Huntsville, AL, USA

Key Points:
- Approximately 10% of TGFs are simultaneous with a distinct and isolated slow low frequency radio pulse
- Simultaneity implies that a TGF source altitude range of 10-15 km is consistent with the analyzed examples
- The consistency of the TGF and radio time scales indicate that the radio pulse is produced directly by the electron acceleration in the TGF production process

Correspondence to:
S. A. Cummer,
cummer@ee.duke.edu

Citation:
Pu, Y., Cummer, S. A., Lyu, F., Briggs, M., Mailyan, B., Stanbro, M., & Roberts, O. (2019). Low frequency radio pulses produced by terrestrial gamma-ray flashes. *Geophysical Research Letters*, *46*, 6990–6997. https://doi.org/10.1029/2019GL082743

Received 8 MAR 2019
Accepted 30 MAY 2019
Accepted article online 5 JUN 2019
Published online 19 JUN 2019

Abstract Do terrestrial gamma-ray flashes (TGFs) produce their own radio signatures? To explore this question, we analyze TGF data from the Fermi Gamma-ray Burst Monitor, independent lightning geolocation data from the National Lightning Detection Network, and low-frequency (LF) magnetic field waveforms, to determine the relationship between TGF generation and LF waveforms. LF waveforms associated with six TGFs are found to contain a clear and isolated slow pulse (~80-μs duration) within a sequence of multiple fast pulses (<10-μs risetime). We find that the slow LF pulse is produced simultaneously with the observed gamma rays, with an uncertainty as small as 7 μs. Simultaneity implies a consistent TGF source altitude range of approximately 10–15 km, which is consistent with previous estimates. These findings provide important evidence that the slow LF pulse, when observed, is associated with TGF production and perhaps produced by the electron acceleration itself.

1. Introduction

Terrestrial gamma-ray flashes (TGFs) are among the most remarkable high energy phenomena in the Earth's atmosphere, producing intense bursts of gamma rays with energies above 20 MeV (Briggs et al., 2010; Fishman et al., 1994; Smith et al., 2005). Relativistic runaway electron avalanches accelerated in strong electric fields inside thunderstorms are the source of gamma-ray production (Dwyer, 2003; Gurevich et al., 1992; Wilson, 1925), but where these strong electric fields are located and how TGFs connect to lightning is not well understood. Using coordinated observations by ground-based radio measurements, from very low frequency to very high frequency, and space-based high-energy radiation detectors from BATSE, RHESSI, and AGILE to Fermi GBM, TGFs were associated from their discovery with thunderstorms (Fishman et al., 1994). Further research connected TGFs to in-cloud lightning discharges (Stanley et al., 2006) and to initial upward in-cloud negative leaders (Cummer et al., 2015; Lu et al., 2010; Lyu et al., 2018; Østgaard et al., 2013; Shao et al., 2010).

Measuring the detailed temporal relationship between TGFs and radio signatures of different lightning processes would improve our understanding of the underlying TGF physics. The simultaneity of TGFs and low frequency radio emissions from lightning was confirmed and narrowed to a few milliseconds in the RHESSI era (Cummer et al., 2005; Stanley et al., 2006) and further reduced to several tens of microseconds after employing data from Fermi GBM in microsecond time precision (Connaughton et al., 2010). Positive polarity energetic in-cloud pulses (+EIPs) when they occur have been found to be all or nearly all upward TGFs (Lyu et al., 2016). However, the converse is not true, and only a small fraction of TGFs are associated with +EIPs. Moreover, the TGF production does not appear to be simultaneous with the +EIP but is instead offset by roughly 10 μs, although this timing relationship has yet to be definitively established. −EIPs are basically identical to +EIPs except for their polarity and thus are conjectured to be linked with downward directed TGFs (Lyu et al., 2015; Lyu & Cummer, 2018). The physics behind the clear statistical EIP-TGF connection are not entirely clear. A more detailed comparison of gamma-ray counts and high time resolution low frequency radio measurements revealed near simultaneity (±18 μs) of gamma-ray production and a slow low-frequency (LF) radio pulse (~50- to 100-μs duration) (Cummer et al., 2011). This connection was reproduced in the context of the feedback TGF model (Dwyer & Cummer, 2013), which predicts that these detectable radio emissions are likely generated by the TGF electron acceleration process itself. This consistency of

model and observation sheds light on the TGF internal physics. However, the relationship between TGF generation and the slow pulse has only been analyzed in detail for a single event and is thus far from definitive as supported by a single event. More observational evidence is needed to determine the validity and universality of such a connection.

Here we aim to better define the time relationship between radio emissions and TGF generation on microsecond timescales, specifically for cases in which there is a clear and isolated slow LF pulse of the type reported by Cummer et al. (2011) in order to establish a statistically robust connection. Combining long-term (2010–2018) TGF data from satellite, data from lightning geolocation networks, and multistation low frequency radio measurements, we find six TGFs that contain an isolate and unique slow LF pulse embedded within the sequence of fast pulses associated with the lightning leader evolution. We find that all six cases show that the slow LF pulse and the TGF production are effectively simultaneous, within the overall timing uncertainty of each event due to lightning location and TGF altitude uncertainties. These measurements produce further evidence that the slow LF pulse, when observed, is a signature of the TGF process.

2. Data and Methods

2.1. Measurements

TGF gamma-ray counts are detected and identified by GBM on the Fermi satellite orbiting at an altitude of about 565 km with inclination of 25.6° (Briggs et al., 2013). GBM consists of 14 scintillation detectors of two types which are, respectively, two bismuth germanate (BGO) detectors (~200 keV–40 MeV) and 12 sodium iodide (NaI) detectors (~8 keV–1 MeV). Because the NaI detectors have longer deadtime for TGF measurements (Briggs et al., 2013) and because many of the TGF photons in the NaI energy range are Compton scattered, producing uncertain delays in their arrival times (Østgaard et al., 2008), we only analyzed counts from the two BGO detectors in this paper. From 16 July 2010, GBM has delivered continuous time-tagged event data with 2-μs time resolution from selected geographic regions and from 26 November 2016 from the entire orbit. Therefore, this work analyzed time-tagged event data from July 2010 to September 2018.

Additionally, ground-based LF observation systems for lightning radio signal detection are deployed around North America (Cummer et al., 2011). The LF sensors are two orthogonal magnetic field coils operating at a bandwidth of approximately 1–300 kHz. In this paper, we analyzed LF data observed from six LF observing sites, which are Duke University (DU; 35.971 °N, −79.094 °E), Florida Institute of Technology (FT; 28.062 °N, −80.624° E), Arecibo, Puerto Rico (PR; 18.370 °N, −66.754 °E), University of Mississippi (MS; 34.364 °N, −89.535 °E), University of Oklahoma (OU; 35.181 °N, −97.440 °E), and Kansas State University (KS; 39.191 °N, −96.584 °E) as shown in the map in Figure 1a. The LF signals are sampled at 1 MHz synchronized by GPS. Simultaneous LF signals can provide details of the TGF associated flashes that help determine the relationship between TGF and certain lightning process.

Moreover, lightning geolocation data from the U.S. National Lightning Detection Network (NLDN) is employed to provide the ground locations of lightning flashes connected to TGFs and help further determine the temporal relationship between LF signals and GBM gamma-ray counts. The location uncertainty of each NLDN-located event with 50% confidence is reported in the data set and will be examined as an important source of TGF-LF timing uncertainty in the following analysis.

2.2. Event Selection

Our goal is to align in time the TGF GBM gamma-ray counts and the ground detected LF signals back propagated in time to the source location of each as determined by NLDN and assess their simultaneity as accurately as possible. The time uncertainty intrinsically in each data set and produced during processing steps will be investigated quantitatively.

The search begins from the Fermi reported TGFs (~2,403 events) from July 2010 to September 2018 in the Americas region. For each event, absolute UT time, the Fermi footprint, and altitude are reported. We search for NLDN lightning events that are possibly connected to these TGFs. NLDN-located events less than 600 km to Fermi footprint (Briggs et al., 2013) and less than 10 ms from the TGF time are considered candidates TGF source flashes. Only 6% (138/2403) of all Fermi TGFs are matched by potential NLDN lightning events. Note that many TGFs occur outside NLDN range. We also require an NLDN to LF sensor distance of less than 800 km to ensure clear and directly arriving ground LF signals, which leaves 72 TGFs.

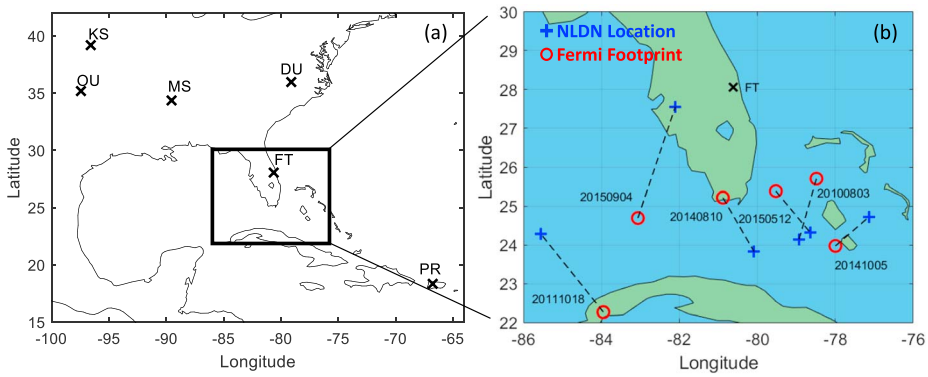

Figure 1. Geographical views of (a) the low-frequency magnetic field sensors and (b) the terrestrial gamma-ray flash footprints and NLDN lightning locations for the six terrestrial gamma-ray flashes analyzed here. NLDN = National Lightning Detection Network.

We next examined the LF waveforms corresponding to those 72 TGFs, looking for clear and isolated slow pulses with pulse duration longer than 50 μs (Cummer et al., 2011; Dwyer & Cummer, 2013) and with minimally overlapping LF radiation pulses so that we can unambiguously connect an LF pulse with the gamma-ray production time. A total of six TGFs with NLDN locations and clear LF slow-pulses were identified, and we investigate these cases in detail in the following analysis. For the remaining 66 events, more than 70% have enough overlapping strong lightning activity (including 13 +EIPs and roughly five unclear but suspected slow pulse cases) occurring around the time of TGF so that it is difficult to distinguish any slow pulse among the overlapping fast lightning pulses. The remaining events show only a weak connection between the TGFs and any lightning pulses, suggesting that the NLDN-identified lightning may not be the source of the TGF.

2.3. Time Alignment Procedure

All data (LF radio signals from one or more sites and associated GBM photon counts) are presented here with time shifted back to the NLDN source location. Here we assume the source altitude of TGF to be 13 ± 3 km. This altitude uncertainty (examined in the following section) will bring a time uncertainty of approximately ±10 μs. With regard to the NLDN location uncertainty, we expanded the semimajor/minor axis of the reported 50% error ellipse by a factor of 3 to yield a 96% confidence lightning location ellipse. Then we picked eight locations distributed equally around the enlarged ellipse and realigned all data based on the eight new NLDN locations. In the following figures, the time alignment based on the originally NLDN location is considered as the baseline, while the alignment from the 8 locations around the ellipse generates the presented time uncertainty due to lightning location uncertainty. The TGF centroid is determined at the time of the median photon count within an episode of "continuous" photon counts which is determined if the time interval of each of two consecutive counts in the episode is less than 20 μs.

3. Analysis and Results

The locations of the six analyzed TGFs are shown in Figure 1, along with the Fermi footprints for each and the location of the nearby LF sensor at Florida Tech. Five of the associated NLDN locations are over water, and one is over land and especially close to the FT sensor. Three of them, labeled with date 20150904, 20140810, and 20100803, are analyzed in detail in the following sections.

3.1. TGF on 4 September 2015

Fermi GBM detected a TGF at 21:23:43.910235 UT on 4 September 2015 (also discussed in Mailyan et al., 2018, and Lyu et al., 2018). The Fermi geographic footprint was 24.69 °N, −83.06 °E while the satellite altitude was 541.55 km. Based on the NLDN search strategy described in section 2, one associated NLDN located lightning event was found at 27.55 °N, −82.10 °E at 21:23:43.908 UT. This event is 331 km horizontally offset from the Fermi footprint and 2.235 ms before the on-orbit TGF detection. LF radio signals associated with this TGF were recorded by five LF sites: FT (156-km range), DU (975 km), OU (1,683 km), PR

(1,873 km), and KS (1,861 km). The NLDN time and approximate location was confirmed by these multisite data.

We now apply the procedure described in section 2 to determine the time alignment at the source location of the gamma ray and radio signals. The source altitudes of both signals are initially assumed to be 13.0 km, which is consistent with observations in Cummer et al. (2015). We also assume the horizontal position of each is the NLDN reported lightning location. We assess the timing uncertainties of these assumptions later in the analysis.

Figure 2 overlays the FT LF signal and gamma-ray counts with time shifted back to source by subtracting wave propagation time from the source to the LF site and to Fermi. The short propagation distance (156 km) from the TGF gives a high amplitude LF signal that is dominated by the ground wave. A sequence of discrete LF pulses starts at 908.0 ms and ends at about 909.5 ms. This pulse sequence is consistent with that produced in an ascending in-cloud leader (Cummer et al., 2015). All of these pulses except for one have a similar shape and fast (<10 μs) risetime.

The unique pulse, from roughly 908.12 to 908.22 ms, is significantly slower than the others (we refer to this feature hereafter as a slow LF pulse). And, importantly, the gamma-ray counts from the Fermi GBM BGO detector are produced at the assumed source location essentially simultaneously with this slow pulse. To better show the timing relationship, an expanded view is shown in Figure 2b. The TGF centroid is determined by the median photon count time and in this case is 908.176 ms. Note that the median count and mean count give essentially identical times in our analysis. We estimate the slow LF pulse centroid through the following procedure. Due to the frequency response of the LF sensor (Cummer et al., 2011), the signal is proportional to dB/dt for pulses with little energy above 100 kHz, like this one. Furthermore, the radiated far-field magnetic field is proportional to the derivative of source current dI/dt, and thus, the LF signal is approximately proportional to d^2I/dt^2. Assuming that the source current is a Gaussian pulse, we fit the measured slow pulse with the second derivative of a Gaussian, which is shown by the cyan dashed curve. This is in good agreement with the measured slow pulse, validating the Gaussian assumption. The full Gaussian current pulse is then shown in cyan with a width of approximately 65 μs determined by ±2 standard deviations with a centroid at 908.176 ms (solid vertical cyan line). There is thus only 2.6 μs time difference between the centroids of the gamma-ray counts and the source current of the slow LF pulse. In other words, the times of the peak gamma-ray production and of the peak source current are effectively simultaneous.

The time alignment here depends critically on the assumed source location, and we estimate the timing uncertainty produced by location uncertainties. The NLDN data report a 50% error ellipse with semiaxes of 0.3 and 0.2 km for this event. Assuming a bivariate Gaussian error distribution with radius, a 3 times larger error ellipse (0.9 and 0.6 km) represents the area in which the lightning occurred with 96% certainty. At eight uniformly spaced locations along the 3 times expanded error ellipse, the distances between the possible lightning location and the two sensor locations (FT LF sensor and Fermi) change so that the centroid time differences also change. These gamma-LF centroid time differences for locations around the ellipse range from −1.7 to +7.0 μs. The resulting timing uncertainty bounds are shown by the vertical dashed magenta lines in Figure 2b. The observed 2.6-μs gamma-LF centroid offset is thus well within the roughly −2 to +7 μs timing uncertainty due to the lightning location uncertainty. Hence, the slow current pulse and the gamma-ray production are effectively simultaneous to within our ability to know the precise source location. This simultaneity is consistent with the idea that the source current is produced by primary and secondary particles in the TGF acceleration process itself (Dwyer & Cummer, 2013). It is also suggested that slow LF pulses, when clearly identifiable, could be a direct signature of TGF production.

3.2. TGFs on 10 August 2014 and 3 August 2010

At 5:49:30.636 UT on 10 August 2014, Fermi GBM recorded a TGF for which the corresponding LF data contains a clear isolated slow pulse. The Fermi footprint at that time was 25.2156 °N, −80.8839 °E, and the satellite altitude was 531.8 km. We again apply the NLDN search procedure as above and find one NLDN-located lightning event at 23.8268 °N, −80.0842 °E at 5:49:30.632 UT, with a horizontal distance of 174 km. Simultaneously, LF signals were detected at four LF sites: FT (472 km), DU (1,350 km), MS (1,485 km), and KS (2,307 km). Figure 3a shows the closest LF waveform (FT) and TGF gamma-ray counts time aligned at the source location over a 5-ms time window. A significant pulse sequence extends from

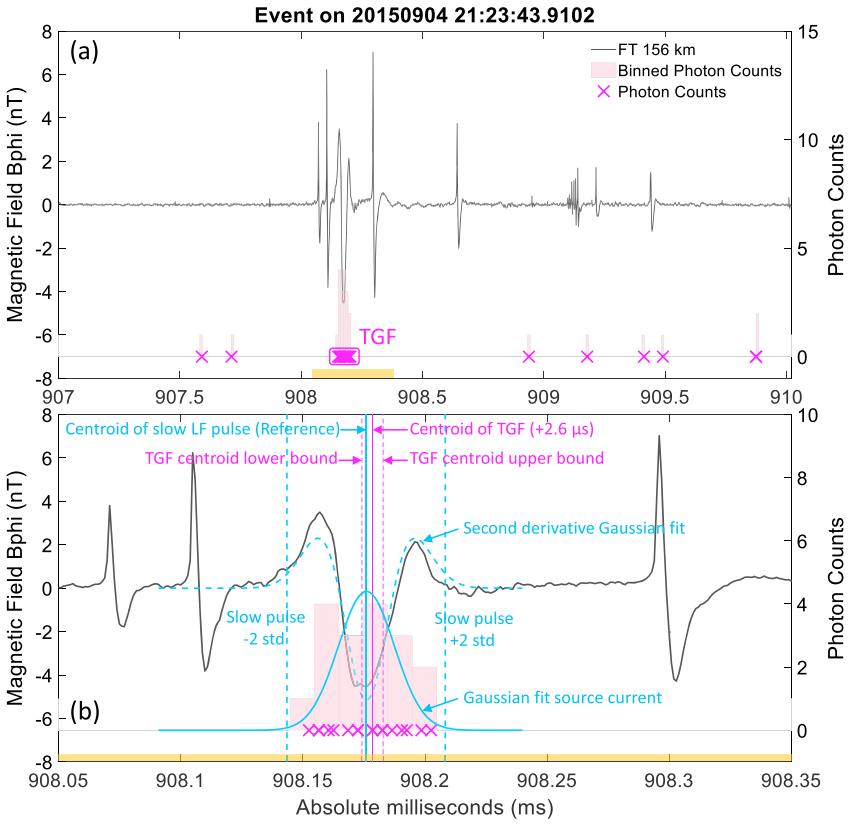

Figure 2. Ground-based LF radio signal from the FT sensor and gamma-ray counts from Fermi Gamma-ray Burst Monitor bismuth germanate with time shifted to National Lightning Detection Network geolocation of a TGF on 4 September 2015. (a) The full event in 3-ms time window. (b) A time-expanded 300-μs view of the slow LF pulse and the associated TGF. Gamma-ray counts are binned to 10 μs (magenta), and the slow LF pulse is fit to a second derivative Gaussian (cyan). The time difference between the TGF and slow LF pulse centroids is 2.6 μs, with uncertainty bounds denoted by two vertical magenta dashed lines considering the uncertainties in National Lightning Detection Network geolocation.

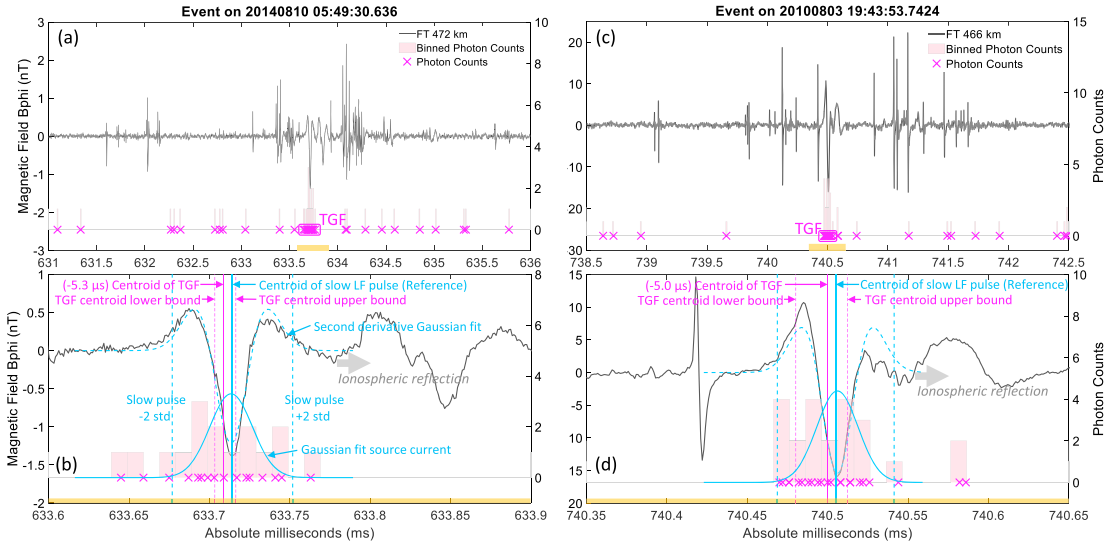

Figure 3. The same as Figure 2 but for (a–b) TGF on 10 August 2014 and (c–d) TGF on 3 August 2010. LF = low frequency; TGF = terrestrial gamma-ray flash.

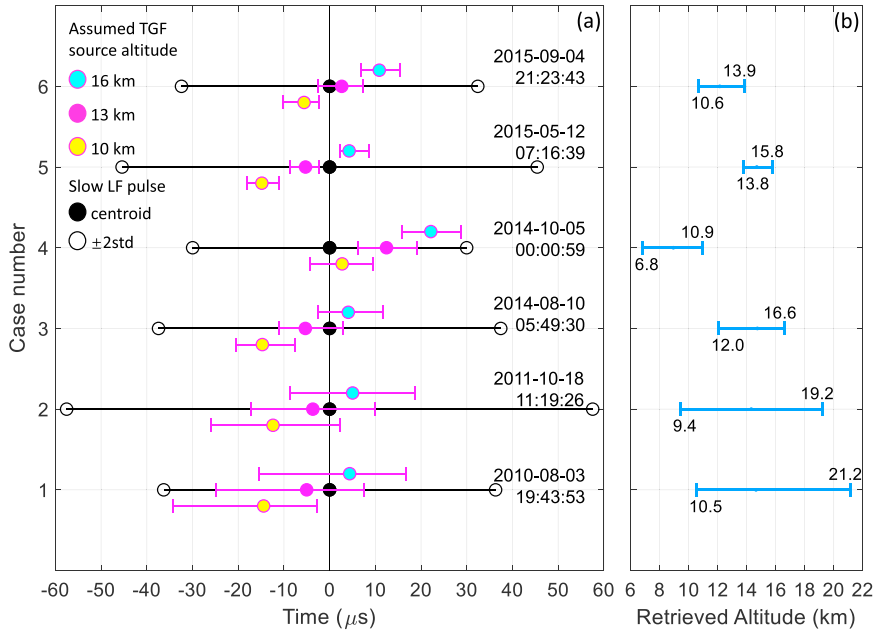

Figure 4. Summary of (a) time alignment results and (b) the estimated source altitude range for all six TGFs associated with an isolated slow LF pulse. The TGF centroid time uncertainty due to National Lightning Detection Network geolocation uncertainty is marked by magenta error bars. Uncertainty in assumed TGF source altitude (10, 13, and 16 km) and its impact on TGF centroid timing is shown in yellow, magenta, and cyan, respectively. The black solid and hollow circles denote the centroid and width of the slow LF pulse, respectively. The estimated TGF source altitude range based on the simultaneity of TGF and slow pulse is shown in blue line for each case. LF = low frequency; TGF = terrestrial gamma-ray flash.

631.5 to 635.5 ms with bursts of fast LF pulses, and there is a single, distinct slow pulse in the middle of that sequence. Note that there is ionospheric reflection following the slow pulse ground wave, marked by a gray arrow in Figure 3b, which should not be regarded as a second independent slow pulse.

We then perform the same detailed timing analysis as that in section 3.1. The time difference between the centroid of the source current pulse and the centroid of the gamma-ray counts is −5.3 μs with an uncertainty of −11/+2 μs due to the NLDN location uncertainty. Both centroids fall within this timing uncertainty, and thus, the slow LF pulse and TGF counts are effectively simultaneous at the source location.

A final example of the isolated slow pulse is evident for the TGF identified by Fermi GBM at 19:43:53.742350 UT, on 3 August 2010. The corresponding Fermi footprint was 25.7025 °N, −78.4847 °E while the on-orbit altitude was 551.15 km. The corresponding NLDN-located lightning was found at 24.1471 °N, −78.9296 °E at 19:43:53.741 UT, resulting in a horizontal distance of 178 km. For this event, LF radio signals were detected at two sites: FT (466 km) and DU (1,312 km). As shown in Figure 3c, the lightning pulse sequence starts around 739 ms and ends at about 741.7 ms also with multiple fast pulses and one isolated slow pulse beginning by 740.45 ms. Once again, when propagation times are accounted for, the burst of gamma-ray counts is effectively simultaneous with the slow pulse at the source location. The time difference between the TGF and the Gaussian fit source current pulse centroids is −5.0 μs, and this falls within the uncertainty window of −25/+7 μs due to the NLDN location uncertainty.

3.3. Summary of All Six Cases

As mentioned in the introduction, another three TGFs, from 12 May 2015 (07:16:39.275 UT), 5 October 2014 (00:00:59.699 UT), and 18 October 2011 (11:19:26.797 UT), met the isolated slow LF pulse selection criteria. The other three cases fundamentally similar to those analyzed in detail in the above. Following the same analysis, all three of these slow pulses are found to be effectively simultaneous with the TGF counts. The overall time relationship between the slow LF pulse and TGF gamma-ray counts for all six cases is summarized in Figure 4a. The time duration of each slow pulse is represented by horizontal black line with a range of 64−116 μs and a mean value of 80 μs. This time scale is considered as the primary characteristic of the slow

LF pulse within a pulse sequence of upward negative leader process. Time shifts due to assumed source altitudes (10, 13, and 16 km) have been examined for each case and marked in different colors. Note that the relative event timing depends linearly on source altitude, and thus, one can deduce the timing implications for the other source altitudes. In four of the six cases, the source altitude assumption of 13 km yields effective simultaneity (within the NLDN location error bars) between the slow pulse and TGF centroids. The other two miss slightly, but Figure 4a shows that small source altitude shifts can result in simultaneity within the uncertainty limits.

The ranges of source altitudes for each event that are consistent with the statistical simultaneity of the TGF and slow LF pulse are shown in Figure 4b. In some cases, the resulting source altitude range is large because of larger NLDN location uncertainties. But the TGF source altitude range of 10–15 km is consistent with all of the events. Note that the TGF source altitude range of 10.6−13.9 km in case 6 is consistent with the LMA VHF source altitudes reported by Mailyan et al. (2018) and Lyu et al. (2018) for the same event.

4. Discussion and Conclusions

In the LF pulse sequence for each of the six TGFs that meet our criteria for analysis, there is a unique slow LF pulse, and the source current moment responsible for this pulse aligns in time with TGF gamma-ray pulse within an as small as 7 μs uncertainty due to lightning location uncertainty. Although it is difficult to define the width of the gamma-ray pulse due to the limited number of counts, Figures 2 and 3 show that the width of the Gaussian fit source current pulse matches well with the width of the continuous episode of discrete gamma-ray counts. These findings suggest that the slow LF pulse, when observable, is simultaneous with and thus linked to the TGF generation process. Moreover, the comparable LF and gamma-ray time scales indicate that this pulse could be the direct radio emissions from the electron acceleration process that produces the TGF (Cummer et al., 2011; Dwyer & Cummer, 2013). The TGF generation process requires upward motion of a relatively large number of energetic electrons. Dwyer and Cummer showed that the motion of the energetic electrons plus secondaries, over a kilometer-scale vertical length and a time scale that matches the TGF, naturally produces an LF pulse with an amplitude and time scale that match observations. The amplitude of the slow pulses here continues to agree well with the predictions of Dwyer and Cummer. Additionally, the smoothness of the slow pulses implies a relatively large number of discrete source particle injections (>104), which is consistent with positron feedback. The consistency with other TGF generation mechanisms is unclear given the lack of quantitative development those theories.

It is worth noting, however, that while the slow LF pulse is reproduced well by a smooth Gaussian source current pulse, the TGF time profiles from the BGO counts are not well fit by Gaussian distributions—they have sharper turn-on and turn-off time scales. It is possible that instrumental effects such as pulse deadtime reduce the number of counts near the centroid in time or that the limited number of counts makes it difficult to determine individual TGF pulse shapes. Further and future analysis of whether and how these two pulse shapes can differ will require further simulation of the TGF process.

One remarkable characteristic of all six cases is that the slow LF pulse is produced in the middle of a sequence of fast pulses and not at the beginning or end. These fast pulses in one case here, on 10 August 2014, were previously analyzed by Cummer et al. (2015; hereafter, C15). That study interpreted the fast pulse sequence as radio emissions from an upward propagating negative leader. The five other cases presented here are essentially identical, further support that at least some TGFs are produced after the leader has initiated but before it reaches its full vertical extent (Cummer et al., 2015).

It should be mentioned that C15 found that the 10 August 2014 TGF was generated when the leader had ascended to 9–10 km, while here the TGF and LF pulse timing indicate a possible TGF altitude range of 12.0 to 16.6 km. These measurements could be consistent if the TGF is produced at altitudes ahead of the leader tip. This would be consistent with the relativistic feedback discharge model (Dwyer, 2012) for TGFs in which relativistic runaway electron avalanche occurs in the large-scale electric field change ahead of the propagating lightning leader. However, a single event containing altitude uncertainties on the order of a few kilometer cannot support such a strong conclusion. Nevertheless, the findings here indicate that TGF source altitudes can be estimated from a timing analysis, and more events in which the lightning leader and TGF altitudes are measured independently could shed light on this important issue.

In conclusion, we have shown that for the fraction (~10%) of TGFs with an LF waveform with clear and isolated slow LF pulse, the slow LF pulse is effectively simultaneous with the observed gamma-ray counts. The timing uncertainty due to the uncertainties of the lightning location is as small as 7 μs. Simultaneity implies a consistent TGF source altitude range of approximately 10–15 km across all events, which is consistent with previous theoretical and experimental expectations. This consistent simultaneity provides further evidence that the slow pulse could be directly produced by the electron acceleration in the TGF production process and is distinct from a traditional lightning process. Collectively, these findings provide new insight into the physics of TGF generation and stimulate further research attention on certain questions as discussed above.

Acknowledgments
The authors would like to acknowledge support from the National Science Foundation Dynamic and Physical Meteorology program through grant AGS-1565606, the Defense Advanced Research Projects Agency (DARPA) Nimbus program through grant HR0011-10-1-0059, and NASA ROSES Fermi Guest Investigation, NNX13AO89G. This work complies with the AGU data policy. The LF waveforms are available on the data repository website (https://doi.org/10.5281/zenodo.3229436). The Fermi BGO photon counts are available at https://heasarc.gsfc.nasa.gov/FTP/fermi/data/gbm/daily/ website. The NLDN data is available at https://www.vaisala.com/en/products/data-subscriptions-and-reports/data-sets/nldn website.

References

Briggs, M. S., Fishman, G. J., Connaughton, V., Bhat, P. N., Paciesas, W. S., Preece, R. D., et al. (2010). First results on terrestrial gamma ray flashes from the Fermi Gamma-ray Burst Monitor. *Journal of Geophysical Research*, *115*, A07323. https://doi.org/10.1029/2009JA015242

Briggs, M. S., Xiong, S., Connaughton, V., Tierney, D., Fitzpatrick, G., Foley, S., et al. (2013). Terrestrial gamma-ray flashes in the Fermi era: Improved observations and analysis methods. *Journal of Geophysical Research: Space Physics*, *118*, 3805–3830. https://doi.org/10.1002/jgra.50205

Connaughton, V., Briggs, M. S., Holzworth, R. H., Hutchins, M. L., Fishman, G. J., Wilson-Hodge, C. A., et al. (2010). Associations between Fermi Gamma-ray Burst Monitor terrestrial gamma ray flashes and sferics from the World Wide Lightning Location Network. *Journal of Geophysical Research*, *115*, A12307. https://doi.org/10.1029/2010JA015681

Cummer, S. A., Lu, G. P., Briggs, M. S., Connaughton, V., Xiong, S. L., Fishman, G. J., & Dwyer, J. R. (2011). The lightning-TGF relationship on microsecond timescales. *Geophysical Research Letters*, *38*, L14810. https://doi.org/10.1029/2011GL048099

Cummer, S. A., Lyu, F., Briggs, M. S., Fitzpatrick, G., Roberts, O. J., & Dwyer, J. R. (2015). Lightning leader altitude progression in terrestrial gamma-ray flashes. *Geophysical Research Letters*, *42*, 7792–7798. https://doi.org/10.1002/2015GL065228

Cummer, S. A., Zhai, Y. H., Hu, W. Y., Smith, D. M., Lopez, L. I., & Stanley, M. A. (2005). Measurements and implications of the relationship between lightning and terrestrial gamma ray flashes. *Geophysical Research Letters*, *32*, L08811. https://doi.org/10.1029/2005GL022778

Dwyer, J. R. (2003). A fundamental limit on electric fields in air. *Geophysical Research Letters*, *30*(20), 2055. https://doi.org/10.1029/2003GL017781

Dwyer, J. R. (2012). The relativistic feedback discharge model of terrestrial gamma ray flashes. *Journal of Geophysical Research*, *117*, A02308. https://doi.org/10.1029/2011JA017160

Dwyer, J. R., & Cummer, S. A. (2013). Radio emissions from terrestrial gamma-ray flashes. *Journal of Geophysical Research: Space Physics*, *118*, 3769–3790. https://doi.org/10.1002/jgra.50188

Fishman, G. J., Bhat, P., Mallozzi, R., Horack, J., Koshut, T., Kouveliotou, C., et al. (1994). Discovery of intense gamma-ray flashes of atmospheric origin. *Science*, *264*(5163), 1313–1316. https://doi.org/10.1126/science.264.5163.1313

Gurevich, A., Milikh, G., & Roussel-Dupre, R. (1992). Runaway electron mechanism of air breakdown and preconditioning during a thunderstorm. *Physics Letters A*, *165*(5-6), 463–468. https://doi.org/10.1016/0375-9601(92)90348-P

Lu, G. P., Blakeslee, R. J., Li, J. B., Smith, D. M., Shao, X. M., McCaul, E. W., et al. (2010). Lightning mapping observation of a terrestrial gamma-ray flash. *Geophysical Research Letters*, *37*, L11806. https://doi.org/10.1029/2010GL043494

Lyu, F., & Cummer, S. A. (2018). Energetic Radio Emissions and Possible Terrestrial Gamma-Ray Flashes Associated With Downward Propagating Negative Leaders. *Geophysical Research Letters*, *45*, 10,764–10,771. https://doi.org/10.1029/2018GL079424

Lyu, F., Cummer, S. A., Briggs, M., Marisaldi, M., Blakeslee, R. J., Bruning, E., et al. (2016). Ground detection of terrestrial gamma ray flashes from distant radio signals. *Geophysical Research Letters*, *43*, 8728–8734. https://doi.org/10.1002/2016GL070154

Lyu, F., Cummer, S. A., Krehbiel, P. R., Rison, W., Briggs, M. S., Cramer, E., et al. (2018). Very high frequency radio emissions associated with the production of terrestrial gamma-ray flashes. *Geophysical Research Letters*, *45*, 2097–2105. https://doi.org/10.1002/2018GL077102

Lyu, F. C., Cummer, S. A., & McTague, L. (2015). Insights into high peak current in-cloud lightning events during thunderstorms. *Geophysical Research Letters*, *42*, 6836–6843. https://doi.org/10.1002/2015GL065047

Mailyan, B. G., Nag, A., Murphy, M. J., Briggs, M. S., Dwyer, J. R., Rison, W., et al. (2018). Characteristics of radio emissions associated with terrestrial gamma-ray flashes. *Journal of Geophysical Research: Space Physics*, *123*, 5933–5948. https://doi.org/10.1029/2018JA025450

Østgaard, N., Gjesteland, T., Carlson, B. E., Collier, A. B., Cummer, S. A., Lu, G., & Christian, H. J. (2013). Simultaneous observations of optical lightning and terrestrial gamma ray flash from space. *Geophysical Research Letters*, *40*, 2423–2426. https://doi.org/10.1002/grl.50466

Østgaard, N., Gjesteland, T., Stadsnes, J., Connell, P., & Carlson, B. (2008). Production altitude and time delays of the terrestrial gamma flashes: Revisiting the Burst and Transient Source Experiment spectra. *Journal of Geophysical Research*, *113*, A02307. https://doi.org/10.1029/2007JA012618

Shao, X. M., Hamlin, T., & Smith, D. M. (2010). A closer examination of terrestrial gamma-ray flash-related lightning processes. *Journal of Geophysical Research*, *115*, A00E30. https://doi.org/10.1029/2009JA014835

Smith, D. M., Lopez, L. I., Lin, R. P., & Barrington-Leigh, C. P. (2005). Terrestrial gamma-ray flashes observed up to 20 MeV. *Science*, *307*(5712), 1085–1088. https://doi.org/10.1126/science.1107466

Stanley, M. A., Shao, X. M., Smith, D. M., Lopez, L. I., Pongratz, M. B., Harlin, J. D., et al. (2006). A link between terrestrial gamma-ray flashes and intracloud lightning discharges. *Geophysical Research Letters*, *33*, L06803. https://doi.org/10.1029/2005GL025537

Wilson, C. T. (1925). *The acceleration of β-particles in strong electric fields such as those of thunderclouds, paper presented at Mathematical Proceedings of The Cambridge Philosophical Society*. Cambridge: Cambridge University Press.